0026-895X/08/7304-1134–1140$20.00
MOLECULAR PHARMACOLOGY
Copyright © 2008 The American Society for Pharmacology and Experimental Therapeutics
Mol Pharmacol 73:1134–1140, 2008

Vol. 73, No. 4
43745/3322243
Printed in U.S.A.

Effects of High-Affinity Inhibitors on Partial Reactions, Charge Movements, and Conformational States of the Ca^{2+} Transport ATPase (Sarco-Endoplasmic Reticulum Ca^{2+} ATPase)

Francesco Tadini-Buoninsegni, Gianluca Bartolommei, Maria Rosa Moncelli, Daniel M. Tal, David Lewis, and Giuseppe Inesi

Department of Chemistry, University of Florence, Sesto Fiorentino, Italy (F.T.-B., G.B., M.R.M.); Department of Biological Chemistry, Weizmann Institute of Science, Rehovot, Israel (D.M.T.); and California Pacific Medical Center Research Institute, San Francisco, California (D.L., G.I.)

Received November 22, 2007; accepted January 22, 2008

ABSTRACT

The inhibitory effects of thapsigargin, cyclopiazonic acid, and 2,5-di(*tert*-butyl)hydroquinone, and 1,3-dibromo-2,4,6-tri(methylisothiouronium)benzene on the Ca^{2+} ATPase were characterized by comparative measurements of sequential reactions of the catalytic and transport cycle, including biochemical measurements and detection of charge movements within a single cycle. In addition, patterns of ATPase proteolytic digestion with proteinase K were derived to follow conformational changes through the cycle or after inhibitor binding. We find that thapsigargin, cyclopiazonic acid, and 2,5-di(*tert*-butyl)hydroquinone inhibit Ca^{2+} binding and catalytic activation as demonstrated with isotopic tracers and lack of charge movement upon addition of Ca^{2+} in the absence of ATP. It has been shown previously that binding of these inhibitors requires the E2 conformational state of the ATPase, obtained in the absence of Ca^{2+}. We demonstrate here that E2 state conformational features are in fact induced by these inhibitors on the ATPase even in the presence of Ca^{2+}. The resulting dead-end complex interferes with progress of the catalytic and transport cycle. Inhibition by 1,3-dibromo-2,4,6-tri(methylisothiouronium)benzene, on the other hand, is related to interference with a conformational transition of the phosphorylated intermediate ($E1{\sim}P \cdot 2Ca^{2+}$ to $E2\text{-}P \cdot 2Ca^{2+}$ transition), as demonstrated by increased phosphoenzyme levels and absence of bound Ca^{2+} translocation upon addition of ATP. This transition includes large movements of ATPase headpiece domains and transmembrane segments, produced through utilization of ATP-free energy as the "conformational work" of the pump. We conclude that the mechanism of high-affinity Ca^{2+} ATPase inhibitors is based on global effects on protein conformation that interfere with ATPase cycling.

The sarco-endoplasmic reticulum Ca^{2+} ATPase (SERCA) is required for active transport of Ca^{2+} into intracellular stores, whereby Ca^{2+} is available for passive release and signaling functions. SERCA is a membrane-bound protein that includes 10 transmembrane helical segments (M1 to M10) and a three-headpiece domain (N, P, and A) protruding from the cytosolic side of the membrane (MacLennan et al., 1985). The ATPase cycle begins with high-affinity binding of two Ca^{2+} ions derived from the cytoplasmic medium ("outside") followed by ATP utilization to form a phosphorylated enzyme intermediate and vectorial transfer of the bound Ca^{2+} into the lumenal medium ("inside"). Hydrolytic cleavage of the phosphoenzyme is the final step that allows the enzyme to undergo a subsequent cycle (Møller et al., 1996). Because of the relatively large distance intervening between the Ca^{2+} binding sites within the transmembrane region and the catalytic site for ATP utilization in the headpiece of the enzyme, coupling of ATP utilization and Ca^{2+} transport requires a "long range intramolecular linkage," which is operated by protein conformational changes (Toyoshima and Inesi, 2004).

Drug interactions with SERCA first came to light when it was discovered that thapsigargin (TG), a plant-derived sesquiterpene lactone (Fig. 1) (Rasmussen et al., 1978; Christensen et al., 1982), produces total and specific Ca^{2+} ATPase inactivation at extremely low concentrations (Lytton et al., 1991; Sagara and Inesi, 1991). TG has become a very useful

This work was supported by the Ente Cassa di Risparmio di Firenze (PROMELAB project), the Ministero dell'Istruzione, dell'Università e della Ricerca (PRIN 2006), and the U.S. National Institutes of Health (R01-HL69830).
Article, publication date, and citation information can be found at http://molpharm.aspetjournals.org.
doi:10.1124/mol.107.043745.

ABBREVIATIONS: TG, thapsigargin; CPA, cyclopiazonic acid; DBHQ, 2,5-di(*tert*-butyl)hydroquinone; TITU, 1,3-dibromo-2,4,6-tri(methylisothiouronium)benzene; SERCA, sarco-endoplasmic reticulum Ca^{2+} ATPase; SSM, solid supported membrane; MOPS, 3-(*N*-morpholino)propanesulfonic acid; SR, sarcoplasmic reticulum; DTT, dithiothreitol; conc., concentration.

tool for experimental manipulations of Ca^{2+} signaling in cells (Hussain and Inesi, 1999) and is presently considered for possible therapeutic applications (Denmeade and Isaacs, 2005; Søhoel et al., 2006). After the discovery of the TG effect, other compounds, such as cyclopiazonic acid (CPA) (Goeger et al., 1988; Seidler et al., 1989), 2,5-di(*tert*-butyl)hydroquinone (DBHQ) (Moore et al., 1987; Murphy et al., 1992), and 1,3-dibromo-2,4,6-tri(methylisothiouronium)benzene (TITU) (Berman and Karlish, 2003; Hua et al., 2005), were found to inhibit SERCA (Fig. 1).

An interesting effect of TG is stabilization of ATPase molecules in ordered arrays (Sagara et al., 1992), thereby facilitating diffraction studies of protein structure. In fact, crystallization of ATPase has been obtained in the absence of Ca^{2+} and in the presence of TG (Toyoshima and Nomura, 2002), demonstrating the TG binding site within a cavity surrounded by the M3, M5, and M7 transmembrane helices near the cytosolic side of the membrane bound region, as also indicated by mutational studies (Zhong and Inesi, 1998; Yu et al., 1999). Crystallographic evidence of CPA and DBHQ bound to SERCA was subsequently obtained, revealing distinct binding sites located near the cytosolic side of the membrane-bound region. CPA resides near the access to the Ca^{2+} sites, locking M1 and M2 against M4 (Moncoq et al., 2007; Takahashi et al., 2007), whereas DBHQ binding is favored by engagement of hydroxyl groups in hydrogen bonding with Asp59 (M1) and Pro308 (M4) and by hydrophobic contacts of butyl groups with neighboring nonpolar residues (Obara et al., 2005). Note that, in all cases, crystallization of ATPase with bound TG, CPA, or DBHQ required a Ca^{2+}-free medium. Crystallization of ATPase in the presence of TITU was never obtained.

With the experiments reported here, we compared systematically the effects of these inhibitors on sequential steps of the catalytic cycle revealed by biochemical and electrical measurements, with conformational effects revealed by changes in exposure of ATPase proteolytic sites to proteinase K in the native membrane environment. In particular, we endeavored to clarify whether long-range effects on protein conformation play an important role in the inhibitory mechanisms of these compounds.

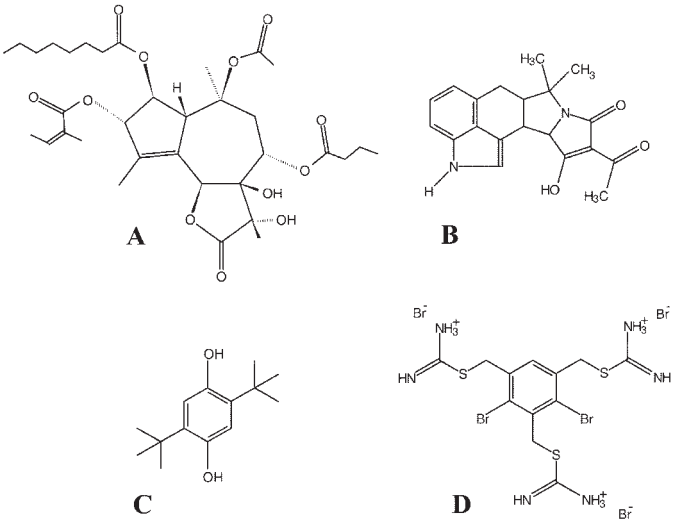

Fig. 1. Structures of inhibitors: TG (A), CPA (B), DBHQ (C), and TITU (D).

Materials and Methods

Reagents. Calcium, potassium, sodium, magnesium chloride, and MOPS were obtained from Merck (Whitehouse Station, NJ) at analytical grade. ATP disodium salt (~97%) and dithiothreitol (DTT, ≥99% purity) were purchased from Fluka (Buchs, Switzerland). Octadecanethiol (98%) from Sigma-Aldrich (St. Louis, MO) was used without further purification. Choline chloride, EGTA, and calcimycin (calcium ionophore A23187) were obtained from Sigma-Aldrich. Potassium oxalate, lithium dodecyl sulfate, sucrose, β-mercaptoethanol, bromphenol blue, and TG were purchased from Sigma-Aldrich. CPA and DBHQ were obtained from BIOMOL Research Laboratories (Exeter, UK). Br-TITU and Br_2-TITU (1.65:1 ratio) were synthesized according to the method of Tal and Karlish (1995). Diphytanoylphosphatidylcholine was purchased from Avanti Polar Lipids (Alabaster, AL) and then solubilized (7.5 mg/ml) in *n*-decane (Merck).

ATPase Preparation. Sarcoplasmic reticulum vesicles were obtained by extraction from the fast-twitch hind-leg muscle of a New Zealand White rabbit, followed by homogenization and differential centrifugation as described by Eletr and Inesi (1972). The vesicles so obtained (light vesicles), derived from longitudinal SR membrane, contained only negligible amounts of the ryanodine receptor Ca^{2+} channel associated with junctional SR.

Functional Measurements. ATPase activity was measured at 25°C in a reaction mixture containing 30 μg/ml SR protein, 50 mM MOPS, pH 7, 50 mM KCl, 3 mM $MgCl_2$, 1 μg of A23187 ionophore, and 2 mM EGTA in the presence or absence of 2 mM $CaCl_2$. The reaction was started by addition of 2 mM ATP, and samples were taken at serial times for Pi determination.

Ca^{2+} binding to the ATPase in the absence of ATP was measured by incubating SR vesicles (40 μg/ml) in 20 mM MOPS, pH 7.0, 80 mM KCl, 5 mM $MgCl_2$, and 10 μM [^{45}Ca]$CaCl_2$. After 5 min of incubation at 25°C, the vesicles were loaded onto 0.45-μm Millipore filters by vacuum suction. The filters were then collected, blotted, and processed for determination of radioactivity.

ATP-dependent Ca^{2+} transport by SERCA was measured at 25°C in a reaction mixture containing 50 mM MOPS, pH 7, 80 mM KCl, 2 mM $MgCl_2$, 50 μg/ml microsomal protein, 5 mM potassium oxalate, and 10 μM free Ca^{2+} with ^{45}Ca tracer. ATP (1 mM) was added to start the reaction, and, at various times a 1-ml reaction mixture was loaded onto a 0.45-μm filter (Millipore, Billerica, MA) by vacuum suction and washed with 15 ml of 2 mM $LaCl_3$ and 10 mM MOPS, pH 7.0. The filter was then processed for determination of radioactivity by scintillation counting.

Enzyme phosphorylation by ATP was measured in an ice-cold reaction mixture containing 50 mM MOPS, pH 7.0, 80 mM KCl, 2 mM $MgCl_2$, 10 μM free Ca^{2+}, and 50 μg/ml microsomal protein. The reaction was started by the addition of 10 μM [γ-^{32}P]ATP and quenched at various times with 1 M perchloric acid. The quenched samples were then loaded onto 0.45-μm Millipore filters by vacuum suction and washed with 15 ml of 0.1 M perchloric acid and 5 ml of cold water. The filters were then processed for determination of radioactivity by scintillation counting.

Measurement of Charge Movements. Charge movements were measured by adsorbing the SR vesicles containing the Ca^{2+}-ATPase onto a mixed alkanethiol/phospholipid bilayer anchored to a gold electrode [the so-called solid supported membrane (SSM)]. The SSM consisted of an octadecanethiol monolayer covalently linked to the gold surface via the sulfur atom with a diphytanoylphosphatidylcholine monolayer on top of it (Pintschovius and Fendler, 1999; Tadini-Buoninsegni et al., 2004).

SR vesicles, after a brief sonication in the absence of detergent, were first adsorbed on the SSM, and the protein was then activated by the rapid injection of a solution containing a suitable substrate (e.g., Ca^{2+} or ATP). If at least one electrogenic step (i.e., a net charge movement across the vesicular membrane generated by the protein) is involved in the relaxation process that follows protein activation,

a current transient can be recorded by the SSM method (Tadini-Buoninsegni et al., 2006). In particular, the electrical response of the ion pump can be monitored under potentiostatic conditions. In this case, movement of a net charge across the activated protein is compensated for by a flow of electrons along the external circuit to keep the applied voltage ΔV constant across the whole metal/solution interphase. The resulting current transient is recorded as a function of time. Normally, experiments are carried out under short circuit conditions (i.e., at zero applied voltage relative to the reference electrode). It should be pointed out that the SSM technique detects pre–steady-state current transients within the first catalytic and transport cycle and is not sensitive to stationary currents after the first cycle. Useful information is gained from current transients. In fact, numerical integration of each transient is related to a net charge movement, which depends upon the particular electrogenic event (i.e., after Ca^{2+} or ATP concentration jumps). In addition, kinetic information can be obtained by fitting the current versus time curves to a sum of exponentially decaying terms. Recently, the traditional SSM method has been robotized and has become commercially available (SURFE^{2}R; IonGate Biosciences GmbH, Frankfurt am Main, Germany).

In all experiments, two buffered solutions were used, the "washing" and the "activating" solution. In Ca^{2+} concentration-jump experiments, the washing solution contained 150 mM choline chloride, 25 mM MOPS, pH 7.0, 0.25 mM EGTA, 1 mM $MgCl_2$, and 0.2 mM DTT. The activating solution contained, in addition, 0.25 mM $CaCl_2$ (10 μM free Ca^{2+}). In ATP concentration-jump experiments, the washing solution contained 150 mM choline chloride, 25 mM MOPS, pH 7.0, 0.25 mM EGTA, 1 mM $MgCl_2$, 0.25 mM $CaCl_2$ (10 μM free Ca^{2+}), and 0.2 mM DTT. The activating solution contained, in addition, 100 μM ATP.

In the experiments with the different inhibitors, the drug was added at the same concentration to both solutions from a stock solution in dimethyl sulfoxide. The concentration-jump experiments have been carried out by using the SURFE^{2}R^{One} device. The SSM sensor, the experimental setup, and the solution exchange technique are described in Kelety et al. (2006).

To verify the reproducibility of the current transients generated within the same set of measurements on the same SSM, each single measurement of the set was repeated 4 to 5 times and then averaged to improve the signal-to-noise ratio. Average standard deviations were usually found to be no more than ±5%.

Free Ca^{2+} concentration was calculated with the computer program WinMAXC (http://www.stanford.edu/~cpatton/winmaxc2.html). Unless otherwise stated, 1 μM A23187, the calcium ionophore, was used to prevent formation of a Ca^{2+} concentration gradient across the SR vesicles. The temperature was maintained at 22–23°C for all the experiments.

Limited proteolytic digestion was performed in reaction mixtures containing 50 mM MOPS, pH 7.0, 50 mM NaCl, 2.0 mM $MgCl_2$, 0.05 mg/ml SR microsomal protein, and 0.05 mg of proteinase K. $CaCl_2$ and EGTA were added as indicated in the figures. After incubation at 25°C for various time intervals, the reaction was quenched with trichloroacetic acid (2.5%), and the protein was solubilized with a medium containing lithium dodecyl sulfate (1%), MOPS (0.312 M), pH 6.8, sucrose (3.75%), β-mercaptoethanol (1.25 mM), and bromphenol blue (0.025%). The samples were then subjected to electrophoretic analysis on 12% gels, and the protein bands were stained with Coomassie Blue R-250. Alternatively, Western blots were obtained using the monoclonal antibody MA3911 or MA3912 (Affinity BioReagents, Golden, CO), followed by goat anti-mouse IgG horseradish peroxidase-conjugated secondary antibodies and visualization with an enhanced chemiluminescence-linked detection system (Pierce, Rockford, IL). The MA3911 antibody reacts preferentially with the amino-terminal region of the ATPase, whereas the MA3912 reacts preferentially with the carboxy-terminal region.

Results

Measurements of ATPase activity were first conducted in the presence of the Ca^{2+} ionophore A23187 to produce passive leak of transported Ca^{2+}, thereby preventing back inhibition by high [Ca^{2+}] buildup in the lumen of the SR vesicles. Linear ATP hydrolysis is obtained under these conditions as a function of time, yielding reliable steady-state rates of ATPase activity in the presence of saturating concentrations of Ca^{2+} and ATP. A comparative evaluation of the concentrations required for inhibition of the Ca^{2+}-ATPase activity by various inhibitors is shown in Fig. 2. As previously reported, the $K_{i,app}$ values vary from the subnanomolar range for TG to 0.05 μM for CPA, 0.48 μM for DBHQ, and 15 μM for TITU (Table 1). It is noteworthy that these are apparent values and may not correspond exactly to the dissociation constants (K_d) of these compounds from the ATPase protein. Steady-state measurement of ATP-dependent Ca^{2+} transport (in the presence of oxalate to obtain linear activity) revealed a pattern of inhibition by TG, CPA, DBHQ, and TITU quite similar to that observed by measurements of ATPase (not shown).

Considering the sequence of partial reactions comprising the catalytic and transport cycle, it was previously observed that TG, CPA, and DBHQ interfere with enzyme activation by Ca^{2+}, thereby preventing ATP utilization and formation of phosphoenzyme intermediate (Table 2). On the other hand, TITU allows Ca^{2+} binding and ATP utilization for formation of phosphoenzyme intermediate (E1P). In fact, in the presence of TITU, phosphorylated enzyme intermediate is formed and rises to nearly match the enzyme stoichiometry. However, its hydrolytic cleavage is sharply reduced (Table 2), and translocation of bound Ca^{2+} does not occur.

An informative method for further characterization of Ca^{2+} transport coupled to ATPase activity is measurement of pre–steady-state charge movements within a single Ca^{2+}-ATPase cycle. The measurements are obtained with vesicular fragments of SR membrane adsorbed on a SSM and subjected to Ca^{2+} jumps in the absence of ATP or to ATP jumps in the presence of Ca^{2+}. Current transients induced by addition of 10 μM Ca^{2+} and subsequent addition of 100 μM ATP in the

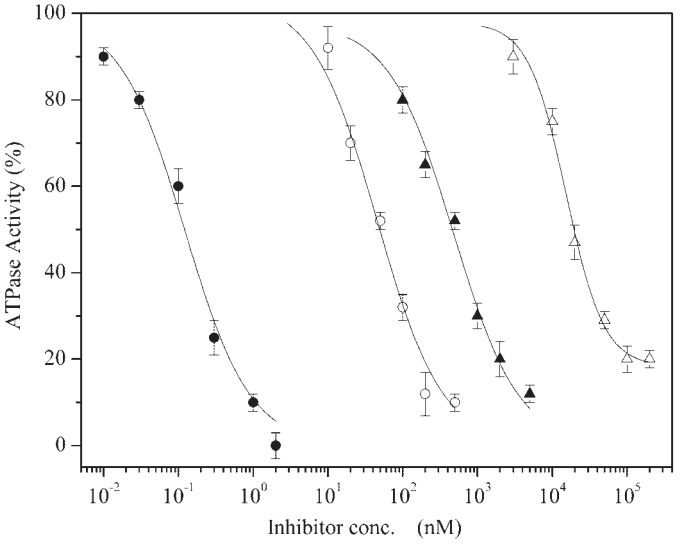

Fig. 2. Effects of various inhibitors on steady-state Ca^{2+}-ATPase activity.

presence of 10 μM Ca^{2+} are shown in Fig. 3. In particular, curve (a) in Fig. 3 represents the initial binding of Ca^{2+} to the ATPase transport sites in the absence of ATP. Curve (b) in Fig. 3 corresponds to the displacement of the bound Ca^{2+} through the ATPase molecule upon utilization of ATP. Each electrogenic event has its own time constant, as shown by the different time frames of the two current transients. Therefore, the charge obtained by numerical integration of each transient is attributed to these sequential electrogenic events, that is, binding of Ca^{2+} to the cytoplasmic sites (Fig. 3, curve a) and vectorial translocation of bound Ca^{2+} after utilization of ATP (Fig. 3, curve b) (Tadini-Buoninsegni et al., 2006). It should be understood that this technique detects single electrogenic steps within the first catalytic and transport cycle and is not sensitive to steady-state events after the first cycle.

Figure 4 shows the dependence of the normalized charges after 10 μM free Ca^{2+} concentration jumps on the concentration of various inhibitors. In each series, these charges were normalized with respect to the maximum charge attained in the absence of the corresponding inhibitor. A sigmoid function was then used to fit the normalized charges as shown in Fig. 4, and the $K_{0.5}$ values for different inhibitors are reported in Table 1. It is shown in Fig. 4 that the charge movement due to Ca^{2+} binding is inhibited strongly by TG, CPA, and DBHQ when these agents are within the concentration range producing ATPase inhibition. The somewhat lower concentration range of CPA producing inhibition of charge movements, relative to steady-state ATPase turnover (compare Fig. 4 with Fig. 2), may be related to the very low quantity of ATPase used in the concentration-jump experiments, because the effective concentration of CPA depends on the protein quantity in the reaction medium (Soler et al., 1998). Most importantly, as opposed to the effects observed with TG, CPA, and DBHQ, the electrogenic event related to Ca^{2+} binding is still retained in the presence of TITU (Fig. 4).

Plots of normalized charges, observed after 100 μM ATP concentration jumps in the presence of 10 μM free Ca^{2+} as a function of the inhibitor concentration, are shown in Fig. 5. Here again the charge was normalized with respect to the maximum charge observed in the absence of the corresponding inhibitor. The $K_{0.5}$ values, which were determined by fitting the normalized charges reported in Fig. 5, are indicated in Table 1. Thus, Fig. 5 shows that all inhibitors, including TITU, interfere with the electrogenic step after addition of ATP and corresponding to translocation of bound Ca^{2+}. It should be pointed out that the effect of the inhibitors on the normalized charge, as shown in Figs. 4 and 5, is simply a reduction of the total charge moved, as reported by integration of the current transients. In particular, in the case of TG, CPA, and DBHQ, it is clear that the lack of translocation signal is related to absence of Ca^{2+} bound to the enzyme (Fig. 4; Table 2). On the other hand, it is apparent that, in the case of TITU, the reduction of the charge is due to direct interference with the translocation step (i.e., phosphoenzyme isomerization), because the Ca^{2+} binding signal is not inhibited by TITU (Fig. 4; Table 2).

The SERCA protein, in the absence or presence of Ca^{2+}, acquires distinct conformations (Fig. 6a) that were characterized by crystallography (Toyoshima et al., 2000; Toyoshima and Nomura, 2002) and correspond to the inactive (E2) or active (E1 · $2Ca^{2+}$) state, respectively. The predominance of these conformational states in the native membrane environment can be determined by following the pattern of proteolytic digestion with proteinase K that is due to exposure or protection of proteolytic sites as a consequence of conformational changes (Danko et al., 2001a,b). In fact, electrophoresis of ATPase protein subjected to limited digestion with proteinase K in the absence of Ca^{2+} shows 95- and 83-kDa bands (Fig. 6, b and c), corresponding to fragments intervening between Lys120 and the carboxyl terminus and Glu243 and the carboxyl terminus. On the other hand, digestion in the presence of 50 μM Ca^{2+} proceeds more rapidly, yielding a prominent 83-kDa band, without a visible 95-kDa band. A small 28-kDa fragment (734/47 to carboxyl terminus) is also noted, depending on the rate of digestion. The presence or absence of the 95-kDa band then reveals whether the digestion occurs with an E2 or an E1 · $2Ca^{2+}$ pattern.

We then performed experiments to obtain ATPase digestion patterns with proteinase K in the presence and in the absence of TG, CPA, DBHQ, and TITU. It is shown in Fig. 6, b and c, that, compared with the nondigested protein (single band), digestion in the absence of drugs yields the patterns described above, distinguished by the presence of the 95-kDa band in the absence of Ca^{2+} and the absence of the 95-kDa band in the presence of Ca^{2+}. Most importantly, however, if TG, CPA, or DBHQ are added, the digestion occurs with the E2 pattern even in the presence of Ca^{2+}. On the other hand, in the presence of TITU, the 95-kDa band is very weak in the absence of Ca^{2+}, and definitely absent in the presence of Ca^{2+}, consistent with a prevalent E1 pattern in the absence of Ca^{2+}, and certainly with a E1.$2Ca^{2+}$ pattern upon addition of Ca^{2+} (Fig. 6, b and c).

Discussion

The discovery of SERCA inhibitors has opened favorable avenues for mechanistic studies on Ca^{2+} homeostasis (Hussain and Inesi, 1999), stereochemistry of drug interactions with proteins (Logan-Smith et al., 2002; Wootton and Michelangeli, 2006; Lape et al., 2008), and possible therapeutic applications (Eckstein-Ludwig et al., 2003; Denmeade and Isaacs, 2005; Søhoel et al., 2006). With the experiments reported here, we endeavored to obtain a comparative characterization of the interactions of four inhibitors with SERCA, their interference with partial reactions of the catalytic and transport cycle, and

TABLE 1
Concentrations of inhibitors producing half maximal inhibition of steady-state ATPase activity, Ca^{2+} binding charge movements, and ATP-dependent Ca^{2+} translocation

	TG	CPA	DBHQ	TITU
	nM		*μM*	
Steady-state activity	0.12 ± 0.02	45 ± 7	0.48 ± 0.05	15 ± 2
Ca^{2+} concentration jumps	0.38 ± 0.06	7.1 ± 0.5	0.18 ± 0.01	
ATP concentration jumps	0.30 ± 0.03	5.1 ± 0.5	0.25 ± 0.02	15 ± 3

the relation of inhibitory mechanisms to protein conformation. In addition to well established methods of functional characterization, in these experiments we have used a novel method to measure charge movements, thereby detecting separately Ca^{2+} binding to the transport sites in the absence of ATP and vectorial translocation of bound Ca^{2+} upon addition of ATP, as sequential electrogenic steps within a single ATPase cycle. In addition, we followed the pattern of ATPase cleavage by proteinase K, thereby determining the conformational state induced by each inhibitor on the ATPase within the native membrane environment.

TABLE 2
Maximal levels of calcium binding in the absence of ATP and phosphoenzyme formation following addition of Ca^{2+} and ATP (nanomoles per milligram of protein)

Sample	Ca^{2+} Binding	Phosphoenzyme
Control	9.2 ± 0.8	1.3 ± 0.3
TG	0	0
TITU	9.0 ± 0.6	3.9 ± 0.2

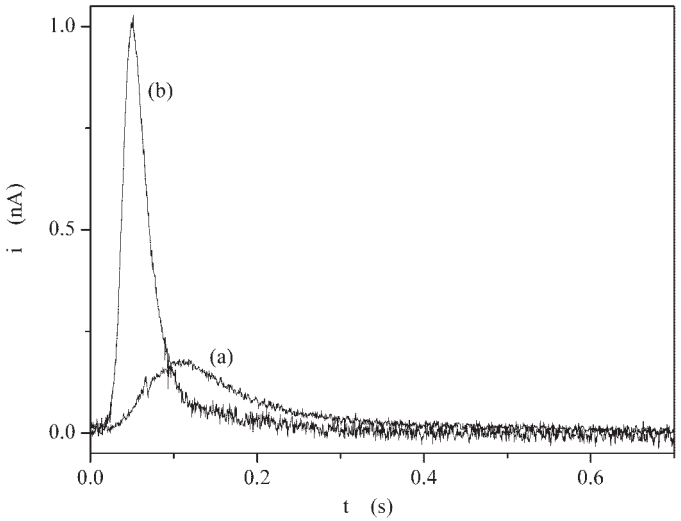

Fig. 3. Current transients induced by a 10 μM free Ca^{2+} concentration jump in the absence of ATP (a) and a 100 μM ATP concentration jump in the presence of 10 μM free Ca^{2+} (b). i, current; t, time.

In accordance with previous reports, we find that TG, CPA, DBHQ, and TITU inhibit SERCA within the nanomolar to micromolar range (Table 1). Both biochemical and electrical measurements demonstrate that TG, CPA, and DBHQ interfere with Ca^{2+} binding (Table 1; Fig. 4), whereby lack of catalytic activation prevents formation of phosphorylated enzyme intermediate (Table 2; Scheme 1). On the contrary, Ca^{2+} binding, catalytic activation, and formation of phosphoenzyme intermediate occur normally in the presence of TITU (Figs. 2 and 4; Table 2). High levels of phosphoenzyme (Table 2), inhibition of ATP-dependent charge movements (Fig. 5), and low cleavage of phosphoenzyme (E1~P) obtained by utilization of ATP are prominent features of TITU inhibition. This, in conjunction with normal cleavage of phosphoenzyme (E2-P) obtained by utilization of Pi (Hua et al., 2005), demonstrates that TITU inhibits the $E1{\sim}P \cdot 2Ca^{2+}$ to $E2\text{-}P \cdot 2Ca^{2+}$ transition (Scheme 1).

A specific feature of the experiments with proteinase K is the diversity of digestion patterns obtained in the presence or absence of Ca^{2+}. This difference is related to the appearance of additional fragments (95 and 14 kDa) as a result of a more favorable exposure of the Leu119/Lys120 site in the E2 configuration (Fig. 6a). This site is located within the M2 helix that extends from the lumen of the SR vesicles to the A domain and is inaccessible to proteinase K in the $E1 \cdot 2Ca^{2+}$ state. On the other hand, in the $E2 \cdot TG$ structure, the Leu119/Lys120 is located within a short helical segment that is evidently accessible to proteinase K as a result of unwinding of the M2 helix around Asn111 and Ala115. The E2 to the E1 patterns of proteolysis by proteinase K are then useful to detect transition of the ATPase conformation from the E1 to the E2 state. It should be understood that, in fact, the digestion pattern characteristic of the E1 conformation is a common feature of sequential states related to H^+ dissociation,

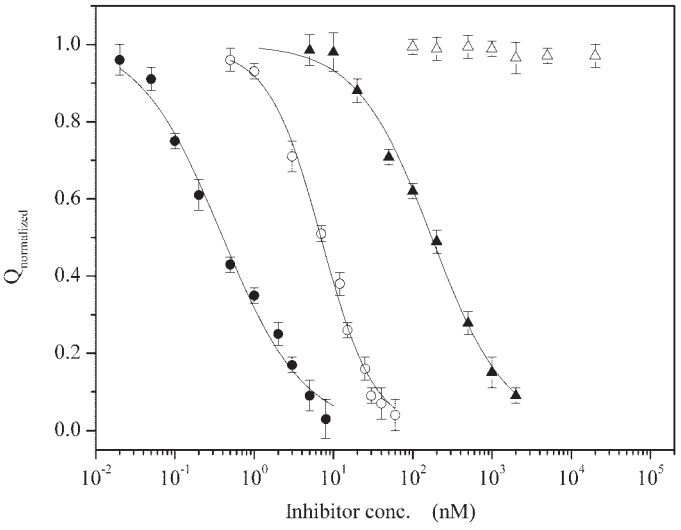

Fig. 4. Dependence of the normalized charge after 10 μM free Ca^{2+} concentration jumps on inhibitor concentration: TG (●), CPA (○), DBHQ (▲), and TITU (△). In each series, the charges are normalized with respect to the maximum charge observed in the absence of the corresponding inhibitor. The solid curves were obtained by fitting with a sigmoid function the normalized charge.

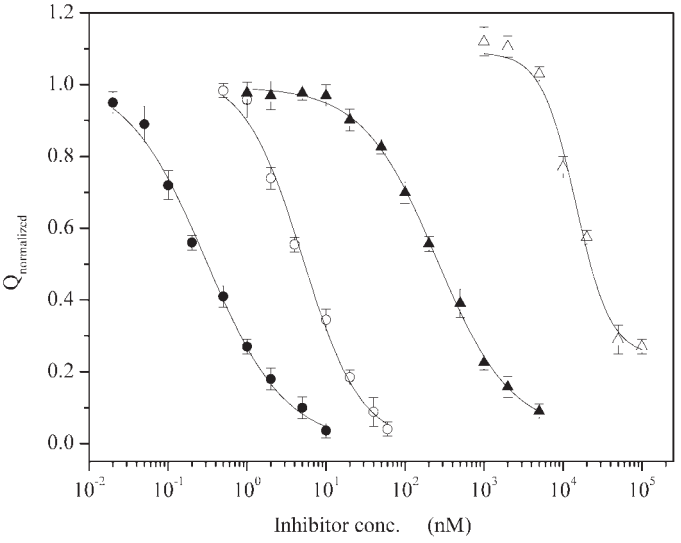

Fig. 5. Dependence of the normalized charge after 100 μM ATP concentration jumps in the presence of 10 μM free Ca^{2+} on inhibitor concentration: TG (●), CPA (○), DBHQ (▲), and TITU (△). In each series, the charges are normalized with respect to the maximum charge observed in the absence of the corresponding inhibitor. The solid curves were obtained by fitting with a sigmoid function the normalized charge.

cooperative binding of 2 Ca^{2+} ions, and catalytic activation (Scheme 1). Most importantly, the proteinase K digestion patterns reveal also the E1-P to E2-P transition, as the A domain undergoes prominent movements, and peptide segments intervening between the A domain and the transmembrane region present variable exposure to proteinase K. Therefore, the proteinase K digestion experiments provide a convenient method to monitor both the E1 to E1-2Ca^{2+} and the E1~P · 2Ca^{2+} to E2-P transitions within the native membrane environment, as the ATPase undergoes the catalytic and transport cycle (Scheme 1).

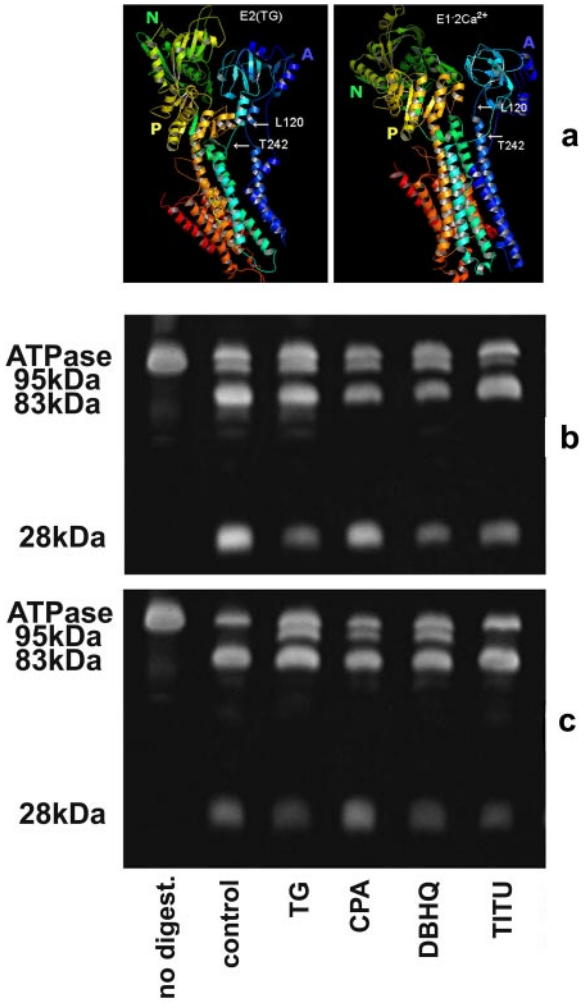

Fig. 6. a, crystallographic models of the Ca^{2+} ATPase in the E2 · TG (left, Protein Data Base code 1iwo) and in the E1 · 2 Ca^{2+} (right, Protein Data Base code 1su4). The sites for initial digestion by proteinase K are in the loops intervening between the A domain and the M2 and M3 transmembrane segments. Note their displacement as the A domain rotates as a consequence of the E1 to E2 transition. Digestion patterns of ATPase with proteinase K in the absence (b) and in the presence of Ca^{2+} (c). The first lane on the left shows a sample with proteinase K denatured before addition of ATPase. The E1 pattern yields complementary 83-kDa (carboxyl terminus) and 28-kDa (amino terminus) bands, whereas the E2 pattern yields additional 95-kDa (carboxyl terminus) and 14-kDa (amino terminus) bands. Note that the E2 pattern is obtained even in the presence of Ca^{2+} when TG (1.0 μM), CPA (10 μM), or DBHQ (20 μM) are added to the reaction mixture, whereas the E1 pattern is obtained in the presence of TITU (100 μM). Digestion (30 min at 25°C) and electrophoresis as explained under *Materials and Methods*. The free Ca^{2+} concentration, when present, was 50 μM. Total protein loaded per well was 30 μg. SERCA protein and fragments thereof were evidenced by Western blotting with specific antibodies. digest., digestion.

We found that, in the presence of TG, CPA, and DBHQ, ATPase digestion with proteinase K yields an E2 pattern even in the presence of Ca^{2+}. This is in agreement with the structures observed under conditions of crystallization in the absence of Ca^{2+} and in the presence of TG, CPA, or DBHQ (Toyoshima and Nomura, 2002; Obara et al., 2005; Moncoq et al., 2007; Takahashi et al., 2007). The crystallographic structures demonstrate that the E2 state favors binding of these inhibitors and define the binding sites. On the other hand, our experiments demonstrate that conformational features of the E2 state are produced in the native membrane environment by TG, CPA, and DBHQ (used separately), even in the presence of Ca^{2+} (Fig. 6, b and c). Therefore, it is clear that the dead-end complex formed by these specific inhibitors is related to a global conformational effect on the ATPase (Wictome et al., 1992; Logan-Smith et al., 2002) whereby catalytic cycling is prevented. It is noteworthy that the conformational state stabilized by the inhibitors is quite similar, but not identical, to the E2 ground state of the physiological ATPase cycle. In fact, local and diverse interactions occur at each inhibitor's binding site. From the functional point of view, lack of reactivity to catalytic ligands and substrate is the most prominent feature distinguishing the dead-end complex from the physiological E2 state.

Contrary to the effects of TG, CPA, and DBHQ, digestion with TITU clearly yields the E1 pattern in the presence of Ca^{2+} (Fig. 6, b and c). This is in agreement with the observation that TITU does not interfere with Ca^{2+} binding, as demonstrated directly with isotopic tracer (Table 2) and by measurements of Ca^{2+}-induced charge movements (Fig. 4). On the other hand, turnover of the phosphoenzyme obtained by utilization of ATP and translocation of bound Ca^{2+} are inhibited by TITU, as demonstrated with isotopic tracer and by measurements of ATP-induced charge movements (Fig. 5). Accumulation of high E1~P · 2Ca^{2+} steady-state levels, in conjunction with normal hydrolytic cleavage of the phosphoenzyme obtained by utilization of Pi (Hua et al., 2005), indicates that the E1~P · 2Ca^{2+} to E2-P · 2Ca^{2+} transition is inhibited by TITU (Scheme 1).

It was reported that, in addition to the Ca^{2+} ATPase, TITU also inhibits the Na^+/K^+ ATPase (Hoving et al., 1995). In the Na^+/K^+ ATPase the mechanism of inhibition is rather complex, including stabilization of the E1 state at low concentrations and stabilization of the E2 state at higher concentrations. On the other hand, inhibition of the Ca^{2+} ATPase occurs prominently through stabilization of the E1 state (see above). It is then apparent that TITU is not strictly specific for the Ca^{2+} pump. It is noteworthy that ATPase crystals with TITU bound within the protein structure were never

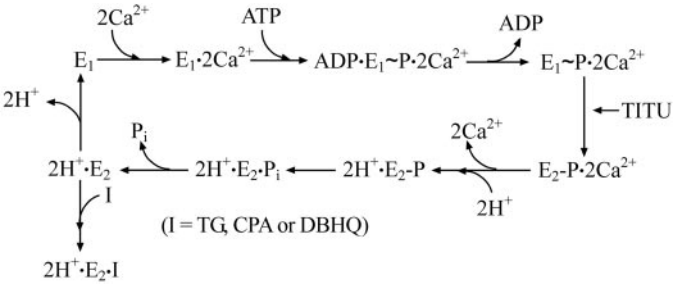

Scheme 1. Sequence of partial reactions in the catalytic and transport cycle of the Ca^{2+} ATPase.

obtained. It is possible that TITU partitions within the membrane phase and then adheres to the membrane-bound enzyme protein, thereby interfering with large movements of the ATPase headpiece domains and transmembrane segments that are required for translocation of bound Ca^{2+} in the normal cycle. These movements, corresponding to the E1~P · $2Ca^{2+}$ to E2-P transition (Toyoshima and Inesi, 2004), represent in fact the "conformational work" of the pump, whereby the free energy of ATP is utilized for reduction of the Ca^{2+} binding affinity and vectorial orientation of the Ca^{2+} binding sites (Inesi et al., 2008). Therefore, conceptually, TITU has a very interesting inhibitory mechanism, which could be referred to as "a stick in the turning wheel of the engine."

In conclusion, our experiments indicate that the mechanism of inhibition involves global effects on protein conformation, resulting in a dead-end complex of the Ca^{2+} ATPase with specific inhibitors such as TG, CPA, and DBHQ. The conformation of the complex is similar (but not identical) to the E2 state (Scheme 1), but its lack of reactivity to ligands and substrate interferes with progress of the catalytic and transport cycle. Inhibition by TITU, on the other hand, is related to interference with conformational transition of the phosphorylated intermediate, as required for energy transduction and active transport of bound Ca^{2+}.

Acknowledgments

We thank Serena Smeazzetto for preliminary SSM measurements on the effect of CPA on charge movements.

References

Berman MC and Karlish SJ (2003) Interaction of an aromatic dibromoisothiouronium derivative with the Ca^{2+}-ATPase of skeletal muscle sarcoplasmic reticulum. *Biochemistry* **42:**3556–3566.

Christensen SB, Larsen IK, Rasmussen U, and Christophersen C (1982) Thapsigargin and thapsigargicin, two histamine liberating sesquiterpene lactones from Tapsia garganica. X-ray analysis of the 7,11-epoxide of thapsigargin. *J Org Chem* **47:**649–652.

Danko S, Daiho T, Yamasaki K, Kamidochi M, Suzuki H, and Toyoshima C (2001a) ADP-insensitive phosphoenzyme intermediate of sarcoplasmic reticulum Ca^{2+}-ATPase has a compact conformation resistant to proteinase K, V8 protease and trypsin. *FEBS Lett* **489:**277–282.

Danko S, Yamasaki K, Daiho T, Suzuki H, and Toyoshima C (2001b) Organization of cytoplasmic domains of sarcoplasmic reticulum Ca^{2+}-ATPase in E_1P and E_1ATP states: a limited proteolysis study. *FEBS Lett* **505:**129–135.

Denmeade SR and Isaacs JT (2005) The SERCA pump as a therapeutic target: making a "smart bomb" for prostate cancer. *Cancer Biol Ther* **4:**14–22.

Eckstein-Ludwig U, Webb RJ, Van Goethem ID, East JM, Lee AG, Kimura M, O'Niel PM, Bray PG, Ward SA, and Krishna S (2003) Artemisinins target the SERCA of Plasmodium falciparum. *Nature* **424:**957–961.

Eletr S and Inesi G (1972) Phospholipid orientation in sarcoplasmic membranes: spin-label ESR and proton MNR studies. *Biochim Biophys Acta* **282:**174–179.

Goeger DE, Riley RT, Dorner JW, and Cole RJ (1988) Cyclopiazonic acid inhibition of the Ca^{2+}-transport ATPase in rat skeletal muscle sarcoplasmic reticulum vesicles. *Biochem Pharmacol* **37:**978–981.

Hoving S, Bar-Shimon M, Tijmes JJ, Goldshleger R, Tal DM, and Karlish SJ (1995) Novel aromatic isothiouronium derivatives which act as high affinity competitive antagonists of alkali metal cations on Na/K-ATPase. *J Biol Chem* **270:**29788–29793.

Hua S, Xu C, Ma H, and Inesi G (2005) Interference with phosphoenzyme isomerization and inhibition of the sarco-endoplasmic reticulum Ca^{2+} ATPase by 1,3-dibromo-2,4,6-tris(methylisothiouronium) benzene. *J Biol Chem* **280:**17579–17583.

Hussain A and Inesi G (1999) Involvement of Sarco/endoplasmic reticulum Ca^{2+} ATPases in cell function and the cellular consequences of their inhibition. *J Membr Biol* **172:**91–99.

Inesi G, Lewis D, Toyoshima C, Hirata A, and de Meis L (2008) Conformational fluctuations of the Ca^{2+} ATPase in the native membrane environment. Effects of pH, temperature, catalytic substrates and thapsigargin. *J Biol Chem* **283:**1189–1196.

Kelety B, Diekert K, Tobien J, Watzke N, Dörner W, Obrdlik P, and Fendler K (2006) Transporter assays using solid supported membranes: a novel screening platform for drug discovery. *Assay Drug Dev Technol* **4:**575–582.

Lape M, Elam C, Versluis M, Kempton R, and Paula S (2008) Molecular determinants of sarco/endoplasmic reticulum calcium ATPase inhibition by hydroquinone-based compounds. *Proteins* **70:**639–649.

Logan-Smith MJ, East JM, and Lee AG (2002) Evidence for a global inhibitor-induced conformational change on the Ca^{2+}-ATPase of sarcoplasmic reticulum from paired inhibitor studies. *Biochemistry* **41:**2869–2875.

Lytton J, Westlin M, and Hanley MR (1991) Thapsigargin inhibits the sarcoplasmic or endoplasmic reticulum Ca-ATPase family of calcium pumps. *J Biol Chem* **266:**17067–17071.

MacLennan DH, Brandl CJ, Korczak B, and Green NM (1985) Amino-acid sequence of a Ca^{2+}+Mg^{2+}-dependent ATPase from rabbit muscle sarcoplasmic reticulum, deduced from its complementary DNA sequence. *Nature* **316:**696–700.

Møller JV, Juul B, and le Maire M (1996) Structural organization, ion transport, and energy transduction of P-type ATPases. *Biochim Biophys Acta* **1286:**1–51.

Moncoq K, Trieber CA, and Young HS (2007) The molecular basis for cyclopiazonic acid inhibition of the sarcoplasmic reticulum calcium pump. *J Biol Chem* **282:**9748–9757.

Moore GA, McConkey DJ, Kass GE, O'Brien PJ, and Orrenius S (1987) 2,5-Di(tert-butyl)-1,4-benzohydroquinone–a novel inhibitor of liver microsomal Ca^{2+} sequestration. *FEBS Lett* **224:**331–336.

Murphy SJ, Schroeder RE, Blacker AM, Krasavage WJ, and English JC (1992) A study of developmental toxicity of hydroquinone in the rabbit. *Fundam Appl Toxicol* **19:**214–221.

Obara K, Miyashita N, Xu C, Toyoshima I, Sugita Y, Inesi G, and Toyoshima C (2005) Structural role of countertransport revealed in Ca^{2+} pump crystal structure in the absence of Ca^{2+}. *Proc Natl Acad Sci U S A* **102:**14489–14496.

Pintschovius J and Fendler K (1999) Charge translocation by the Na^+/K^+-ATPase investigated on solid supported membranes: rapid solution exchange with a new technique. *Biophys J* **76:**814–826.

Rasmussen U, Christensen SB, and Sandberg F (1978) Thapsigargine and thapsigargicine, two new histamine liberators from Tapsia garganica L. *Acta Pharm Suec* **15:**133–140.

Sagara Y and Inesi G (1991) Inhibition of the sarcoplasmic reticulum Ca^{2+} transport ATPase by thapsigargin at subnanomolar concentrations. *J Biol Chem* **266:**13503–13506.

Sagara Y, Wade JB, and Inesi G (1992) A conformational mechanism for formation of a dead-end complex by the sarcoplasmic reticulum ATPase with thapsigargin. *J Biol Chem* **267:**1286–1292.

Seidler NW, Jona I, Vegh M, and Martonosi A (1989) Cyclopiazonic acid is a specific inhibitor of the Ca^{2+}-ATPase of sarcoplasmic reticulum. *J Biol Chem* **264:**17816–17823.

Søhoel H, Jensen AM, Møller JV, Nissen P, Denmeade SR, Isaacs JT, Olsen CE, and Christensen SB (2006) Natural products as starting materials for development of second-generation SERCA inhibitors targeted towards prostate cancer cells. *Bioorg Med Chem* **14:**2810–2815.

Soler F, Plenge-Tellechea F, Fortea I, and Fernandez-Belda F (1998) Cyclopiazonic acid effect on Ca^{2+}-dependent conformational states of the sarcoplasmic reticulum ATPase. Implication for the enzyme turnover. *Biochemistry* **37:**4266–4274.

Tadini-Buoninsegni F, Bartolommei G, Moncelli MR, Inesi G, and Guidelli R (2004) Time-resolved charge translocation by sarcoplasmic reticulum Ca-ATPase measured on a solid supported membrane. *Biophys J* **86:**3671–3686.

Tadini-Buoninsegni F, Bartolommei G, Moncelli MR, Guidelli R, and Inesi G (2006) Pre-steady state electrogenic events of Ca^{2+}/H^+ exchange and transport by the Ca^{2+}-ATPase. *J Biol Chem* **281:**37720–37727.

Takahashi M, Kondou Y, and Toyoshima C (2007) Interdomain communication in calcium pump as revealed in the crystal structures with transmembrane inhibitors. *Proc Natl Acad Sci U S A* **104:**5800–5805.

Tal DM and Karlish SJD (1995) Synthesis of a novel series of arylmethylisothiouronium derivatives. *Tetrahedron* **51:**3823–3830.

Toyoshima C, Nakasako M, Nomura H, and Ogawa H (2000) Crystal structure of the calcium pump of sarcoplasmic reticulum at 2.6 Å resolution. *Nature* **405:**647–655.

Toyoshima C and Nomura H (2002) Structural changes in the calcium pump accompanying the dissociation of calcium. *Nature* **418:**605–611.

Toyoshima C and Inesi G (2004) Structural basis of ion pumping by Ca^{2+}-ATPase of the sarcoplasmic reticulum. *Annu Rev Biochem* **73:**269–292.

Wictome M, Michelangeli F, Lee AG, and East JM (1992) The inhibitors thapsigargin and 2,5-di(tert-butyl)-1,4-benzohydroquinone favour the E2 form of the Ca^{2+}, Mg^{2+}-ATPase. *FEBS Lett* **304:**109–113.

Wootton LL and Michelangeli F (2006) The effects of the phenylalanine 256 to valine mutation on the sensitivity of sarcoplasmic/endoplasmic reticulum Ca^{2+} ATPase (SERCA) Ca^{2+} pump isoforms 1, 2, and 3 to thapsigargin and other inhibitors. *J Biol Chem* **281:**6970–6976.

Yu M, Lin J, Khadeer M, Yeh Y, Inesi G, and Hussain A (1999) Effects of various amino acid 256 mutations on sarcoplasmic/endoplasmic reticulum Ca^{2+} ATPase function and their role in the cellular adaptive response to thapsigargin. *Arch Biochem Biophys* **362:**225–232.

Zhong L and Inesi G (1998) Role of the S3 stalk segment in the thapsigargin concentration dependence of sarco-endoplasmic reticulum Ca^{2+} ATPase inhibition. *J Biol Chem* **273:**12994–12998.

Address correspondence to: Dr. Maria Rosa Moncelli, Department of Chemistry, University of Florence, Via della Lastruccia 3, 50019 Sesto Fiorentino, Florence, Italy. E-mail: moncelli@unifi.it